

UNIVERSITY OF CALIFORNIA AT BERKELEY ASTRONOMY DEPARTMENT

THE *ASCA* X-RAY SPECTRUM OF THE BROAD-LINE RADIO GALAXY PICTOR A: A SIMPLE POWER LAW WITH NO Fe K α LINE

MICHAEL ERACLEOUS^{1,2} AND JULES P. HALPERN³

To appear in *The Astrophysical Journal*

ABSTRACT

We present the X-ray spectrum of the broad-line radio galaxy Pictor A as observed by *ASCA* in 1996. The main objective of the observation was to detect and study the profiles of the Fe K α lines. The motivation was the fact that the Balmer lines of this object show well-separated displaced peaks, suggesting an origin in an accretion disk. The 0.5–10 keV X-ray spectrum is described very well by a model consisting of a power law of photon index 1.77 modified by interstellar photoelectric absorption. We find evidence for neither a soft nor a hard (Compton reflection) excess. More importantly, we do not detect an Fe K α line, in marked contrast with the spectra of typical Seyfert galaxies and other broad-line radio galaxies observed by *ASCA*. The 99%-confidence upper limit on the equivalent width of an unresolved line at a rest energy of 6.4 keV is 100 eV, while for a broad line ($FWHM \approx 60,000 \text{ km s}^{-1}$) the corresponding upper limit is 135 eV. We discuss several possible explanations for the weakness of the Fe K α line in Pictor A paying attention to the currently available data on the properties of Fe K α lines in other broad-line radio galaxies observed by *ASCA*. We speculate that the absence of a hard excess (Compton reflection) or an Fe K α line is an indication of an accretion disk structure that is different from that of typical Seyfert galaxies, e.g., the inner disk may be an ion torus.

Subject headings: accretion, accretion disks – galaxies: active – galaxies: individual (Pictor A) – galaxies: nuclei – line: profiles – X-rays: galaxies

¹ Hubble Fellow

² Department of Astronomy, University of California, Berkeley, CA 94720, mce@beast.berkeley.edu

³ Columbia Astrophysics Laboratory, Columbia University, 550 West 120th Street, New York, NY 10027, jules@astro.columbia.edu

1. INTRODUCTION

The observed X-ray spectra of (radio-quiet) Seyfert galaxies have been interpreted for almost a decade as a combination of a power-law continuum which is seen directly and its reflection from cool, dense matter (e.g., Pounds et al. 1987; Turner & Pounds 1989; Nandra & Pounds 1994). The power-law continuum is generally thought to be the primary radiation from an X-ray source associated with the inner parts of the accretion disk while the reflecting medium is believed to be the accretion disk itself – the only structure in the vicinity of the X-ray source thought to have a Thompson optical depth greater than unity (George, Nandra, & Fabian 1991; George & Fabian 1991; Matt, Perola, & Piro 1991; but see also Nandra & George 1994 for a possible alternative, inspired by the ideas of Guilbert & Rees). The reflected X-rays manifest themselves as a flattening of the spectrum at energies higher than 10 keV, and as a number of fluorescent lines, the most prominent of which is Fe K α at 6.4–6.9 keV (the exact energy depending on the ionization state of the disk). The recent detection of extremely broad ($FWZI \sim 0.3 c$), asymmetric Fe K α lines in the spectra of Seyfert galaxies by *ASCA* bolsters the above picture since their profiles conform to relativistic disk kinematics (Mushotzky et al. 1995; Tanaka et al. 1995; Nandra et al. 1997a). The observed X-ray spectroscopic properties have led to models for the structure of the inner accretion disk involving a hot corona overlaying an optically thick, geometrically thin disk (Haardt & Maraschi 1991, 1993; Haardt, Maraschi, & Ghisellini 1994; Sincell & Krolik 1997). X-ray photons produced in the corona are reflected by the underlying cool disk producing the reflected continuum in the strength necessary to explain the observations.

The radio-loud analogs of Seyfert galaxies, the broad-line radio galaxies (hereafter BLRGs) are considerably less numerous and hence have not been studied as extensively. Nevertheless, several indications suggest that the central engines of BLRGs (and possibly their entire accretion flows) are systematically different from those of Seyfert galaxies. The most obvious, and yet not duly appreciated, difference is the ability of the central engines of BLRGs to accelerate and collimate powerful relativistic jets. A more subtle, but still significant, difference is that the *optical* emission lines of BLRGs are about twice as broad as and considerably more structured than those of Seyfert galaxies (Miley & Miller 1979; Steiner 1981). Unlike Seyfert galaxies, about 10% of BLRGs feature double-peaked Balmer lines which are characteristic of accretion disk dynamics (Eracleous & Halpern 1994). Moreover, the line-emitting gas in the nuclei of BLRGs is thought to be preferentially confined to a plane perpendicular to the axis of the radio jet (Wills & Browne 1986; Jackson & Browne 1990), and synthetic line profiles computed under this assumption match the observed profiles quite well (Jackson, Penston & Pérez 1991; Corbin 1997; Eracleous & Halpern 1998a). From a theoretical perspective, it has long been suspected that the inner accretion disks of BLRGs are hot, ion-supported tori³ (Rees et al. 1982) rather than disk-corona sandwiches as proposed for Seyferts. If so, only the outer disk at radii $r \gtrsim 300 r_g$ ($r_g \equiv GM/c^2$) would be able to reflect the primary X-rays with the main consequence that the reflected continuum and the Fe K α lines should be considerably weaker in BLRGs than in Seyferts. Indeed, the available data support this view. As shown first by Zdziarski et al. (1995) and verified later by Woźniac et al. (1998) the X-ray spectra of BLRGs have considerably weaker and narrower Fe K α lines and a reflected continuum consistent with zero (but see also our later discussion in §4.1). To reconcile the fact that Fe K α lines are detected in the spectra of BLRGs but a reflected continuum is not, Woźniac et al. (1998) suggest that there is no medium in the vicinity of the primary X-ray source that can act as an efficient reflector. Instead, they propose that the Fe K α lines originate in matter of moderate

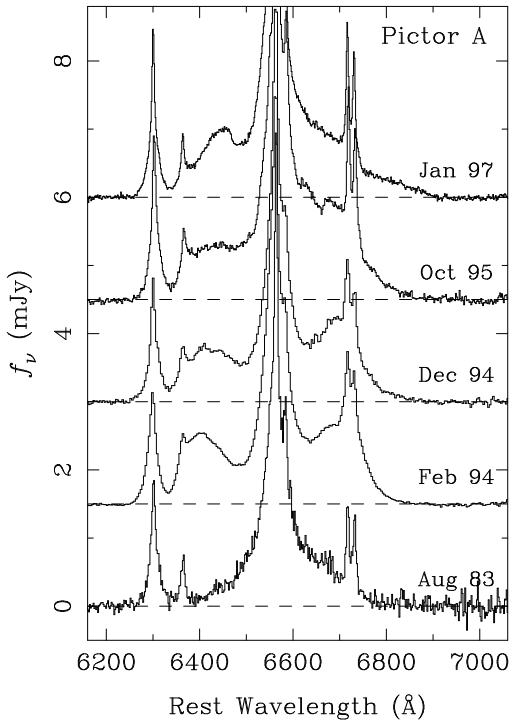


FIGURE 1. – A compilation of H α spectra of Pictor A spanning the past 3 years, along with a spectrum from 1983 showing the H α profile before the appearance of the displaced peaks. The horizontal dashed lines mark the zero level of each spectrum. Although the profile has been varying over the past few years, the displaced peaks were certainly present at the time of the *ASCA* observation in 1996 November.

column density (of order 10^{23} cm $^{-2}$) at a large distance from the X-ray source, where reflection is inefficient.

We have been observing BLRGs with *ASCA* with one of our main goals the investigation of possible differences between the structure of their inner accretion disks and those of Seyfert galaxies. As such, our study complements the work on the X-ray spectra and Fe K α lines of Seyferts by Tanaka et al. (1995), Mushotzky et al. (1995), and Nandra et al. (1997a). We note parenthetically that the fact that a fair fraction of BLRGs display superluminal motions is very useful from a practical perspective because the apparent superluminal speed yields a stringent upper limit on the inclination of the jet (and hence the disk) to the line of sight. The inclination of the disk is an important parameter in the calculation of the model X-ray spectrum. Another important aim of our program is to use the properties of the Fe K α lines to test models for the origin of the double-peaked Balmer lines in BLRGs. The latter goal is closely related to the former since one possible (and very likely) origin of the double-peaked Balmer lines is the accretion disk itself. In fact, the line-emitting disk model of Chen & Halpern (1989) invokes an ion torus in the inner disk which has a large vertical extent and illuminates the outer disk effectively and drives the Balmer-line emission. Accordingly, we have targeted BLRGs which are bright X-ray sources and have double-peaked emission lines. In an earlier paper (Eracleous, Halpern, & Livio 1996) we reported the results of our observation of 3C 390.3, a BLRG with *persistent* double-peaked Balmer lines. We found a resolved Fe K α line in 3C 390.3 with a *FWHM* of 15,000 km s $^{-1}$ (similar to the width of the Balmer lines) and most likely coming from an accretion disk at a characteristic radius of $250 r_g$. The relatively large radius of the line-emitting region is consistent with the ion torus

³ The ion torus is very similar to what is known today as an advection-dominated accretion flow (Narayan & Yi 1994, 1995)

hypothesis discussed above. Both the Balmer lines and the Fe K α line could be coming from the same region in the outer disk.

In this paper we present the X-ray spectrum of the BLRG Pictor A, obtained recently with *ASCA*, and we analyze its *ROSAT* PSPC spectrum retrieved from the *ROSAT* public archive. Pictor A’s claim to fame is the abrupt appearance of double-peaked Balmer lines sometime in the mid-1980s (Halpern & Eracleous 1994; Sulentic et al. 1995). The evolution of the H α line profile since the discovery of the double-peaked lines is depicted in Figure 1. Although the H α line *profile* has been varying over the past few years, it has maintained its overall double-peaked shape and was present at the time of the *ASCA* observation. Because double-peaked emission lines are often considered to originate in an accretion disk we thought it likely that the Fe K α line would have the same profile. The separation of the displaced peaks in the Balmer lines is of order 14,000 km s $^{-1}$, which is within the resolution of the *ASCA* SIS, making Pictor A an attractive target. Much to our surprise, however, we do not detect a strong Fe K α line in Pictor A at all. To explore the implications of this result we compare the Fe K α properties of Pictor A with those of other BLRGs and Seyfert 1 galaxies observed by *ASCA*. In §2 we describe the data and the preliminary reductions, while in §3 we compare the observed spectra with models and with the results of earlier X-ray observations of Pictor A. In §4 we place the X-ray properties of Pictor A in the context of the X-ray properties of BLRGs and we compare them with those of Seyferts. We discuss possible reasons for the weakness of the Fe K α line and the implications for the structure of the central engines of BLRGs. In §5 we summarize our conclusions and present our final speculations. Throughout this paper we assume a Hubble constant $H_0 = 50$ km s $^{-1}$ Mpc $^{-1}$ and a deceleration parameter $q_0 = 0$.

2. DATA AND PRELIMINARY REDUCTIONS

Pictor A was observed with *ASCA* (Tanaka, Inoue, & Holt 1994) on 1996 November 23–26, with the SIS detectors in 1-CCD FAINT mode and with the GIS detectors in PH mode. The data were reduced in a standard manner, as described by Eracleous et al. (1996); we refer the reader to this paper for all details associated with the data reduction as well as the subsequent model fitting. In summary, the detected photons were screened to eliminate events recorded while the telescope was pointing very close to the limb of the Earth or events recorded immediately before or after passage through the South Atlantic Anomaly or the day/night terminator. Because the original data were taken in FAINT mode, we were also able to correct the dark-frame error and the echo effect in the SIS detectors. All of the above tasks were carried out using the XSELECT/FTOOLS software package (Blackburn, Greene, & Pence 1994; Ingham 1994). Source spectra and light curves were extracted from a circular (GIS) or rectangular (SIS) regions centered on the source and large enough to encompass the entire point-spread function. Background spectra and light curves were also extracted from annuli around the source. The effective exposure time and source count rate for each detector are summarized in Table 1. The source and background light curves were inspected for variability on time scales ranging from 15 minutes to the length of the observation and none was found.

ROSAT observed Pictor A with its PSPC twice, first during its All-Sky Survey (RASS) in the second half of 1990, and then in a pointed observation on 1991 February 18. Results from the RASS observation are reported by Brinkman & Siebert (1994); we include their reported exposure time and count rate in Table 1 for completeness. We were able to retrieve the data from the second, pointed observation from the public archive and use them along with the *ASCA* data in our analysis. As with the *ASCA* data we extracted a PSPC source light curve and spectrum from a circular region of radius 75'' centered on the source, as well as a background light curve and spectrum from an annulus around the source. The effective exposure time and count rate are reported in Table 1.

TABLE 1: EXPOSURE TIMES AND COUNT RATES

Detector	Year	Exposure Time (s)	Source Count Rate ^a (s ⁻¹)	Background/Source
<i>ASCA</i> /SIS 0	1996	61,877	0.56	0.092
<i>ASCA</i> /SIS 1	1996	61,563	0.43	0.073
<i>ASCA</i> /GIS 2	1996	68,790	0.30	0.096
<i>ASCA</i> /GIS 3	1996	68,762	0.36	0.105
<i>ROSAT</i> /PSPC	1991	4,405	0.78	0.027
<i>ROSAT</i> /PSPC ^b	1990	510	0.63	...

^a The SIS, GIS, and PSPC count rates refer to the energy ranges 0.6–8.0 keV, 0.9–10.0 keV and 0.1–2.3 keV, respectively.

^b RASS observation (Brinkmann & Siebert 1994).

Although there was no discernible source variability within the *ROSAT* observation, the soft X-ray flux measured by the PSPC is approximately a factor of 3 higher than the soft X-ray flux measured by the *ASCA* detectors in the same bandpass. This long-term variability, which comes as no surprise, is quantified and discussed below.

3. COMPARISON OF THE OBSERVED SPECTRUM WITH MODELS

3.1 The Shape of the Continuum

The shape of the continuum is best described by a simple power law modified by interstellar photoelectric absorption³. The spectra of Seyfert galaxies and some BLRGs often include an Fe K α line at a rest energy of 6.4 keV, which can be modeled (at least at first) by assuming a Gaussian line profile. In our effort to model the continuum of Pictor A we start with the simplest possible model, the power law, and then we examine whether more components are needed. We have investigated whether the data allow for an additional spectral component at low energies (a soft excess) by adding it to the model and looking for a significant improvement in the fit. We found no evidence for a soft excess regardless of what model we used to describe it (broken power law, bremsstrahlung, or blackbody).

The shape of the X-ray continuum of Seyfert galaxies is observed to deviate from a simple power law at energies above 10 keV, which has been interpreted as the result of an additional spectral component, arising from Compton reflection of the “primary” X-rays from cool dense matter (see §1). The contribution of the Compton-reflected X-rays is expected to be small at energies below 10 keV, but we have searched for it in the GIS spectra, nevertheless. To determine whether this additional component is present, we fitted the 2.0–10.0 keV GIS spectra together using a model comprising a power-law spectrum and its Compton reflection from a slab of cool dense matter

³ Model fits to the continuum were carried out using the XSPEC software package (Arnaud 1996), adopting the photoelectric absorption cross-sections of Morrison & McCammon 1983. We used version 4 (March 3, 1995) of the GIS response matrices, while for the SIS data we use response matrices created specifically for this observation, taking into account the evolution of the detector properties.

(Lightman & White 1989), which could be the accretion disk. The free parameters of the model, in addition to the power-law index and normalization, are the inclination angle of the slab to the line of sight and the solid angle it subtends to the primary X-ray source. The iron abundance in the slab was assumed to be solar and the primary continuum was assumed to be cut off exponentially at 300 keV. The spectrum of reflected X-rays was computed as a function of inclination angle using the transfer functions of Magdziarz & Zdziarski (1995). The result of this investigation is that a spectral component arising from Compton reflection is *not* required by the data. By varying the inclination and solid angle of the reflecting slab over the entire range of allowed values we find that the fit to the data does not improve significantly, which implies that the two parameters are formally unconstrained (the significance of the improvement never exceeds 68%, or ‘1 σ ’, for 2 interesting parameters).

By fitting the observed distribution of counts per energy channel from each instrument separately we derive model parameters which are consistent with each other, and thus we justify carrying out joint fits to the data from the two SIS detectors and similarly to the data from the two GIS detectors. We find a discrepancy between the model and the SIS 1 data at energies between 0.5 and 1 keV. By ignoring this region of the SIS 1 spectrum we obtain a good fit with consistent parameters to data from all instruments individually, and to data from pairs of instruments fitted simultaneously. Therefore, we adopted this empirical remedy. We note in defense of our approach that Yaqoob (1996) finds the same systematic discrepancy that we do using two separate observations of 3C 273 taken during the performance verification phase and during cycle 4. The parameters describing the best-fitting model are summarized in Table 2. The weighted mean power-law index determined from the SIS and GIS spectra is 1.77 ± 0.03 and the equivalent hydrogen column density of absorbing matter is $(6 \pm 2) \times 10^{20} \text{ cm}^{-2}$, as measured by the SIS detectors, which are the most sensitive at low energies (all error bars correspond to the 99% confidence limits for 2 interesting parameters). The spectra of counts per energy channel from the GIS and SIS detectors are shown in Figure 2a, b. The model spectra, after convolution with the telescope and detector response matrices are overlayed for comparison. The uncertainties in the best-fitting model parameters can also be expressed graphically in terms of the 99% confidence contours in a 2-parameter plane, as shown in Figure 3. The GIS and SIS confidence contours overlap at the 90% and 99% confidence levels indicating that the results from the two sets of detectors are consistent with each other.

The *ROSAT* PSPC spectrum was fitted separately using the same model as the one used for the *ASCA* spectra. The spectrum and best-fitting model are shown in Figure 2c, while the best-fitting model parameters and their uncertainties are included in Table 2. The model that describes the *ROSAT* spectrum is consistent, within uncertainties, with the model describing the *ASCA* spectra, save for the normalization. This is illustrated in Figure 3, where the 99% confidence contour for the parameters of the *ROSAT* spectrum is compared to the corresponding contours deprived for the *ASCA* spectra. The difference in model normalizations between the *ROSAT* and *ASCA* spectra is reflected in the 0.7–2.4 keV fluxes reported in Table 2 (this band was chosen because it is common to the *ROSAT* PSPC and the *ASCA* SIS). The flux appears to have increased by a factor of 2.6 between 1991 and 1996, which is most likely the result of intrinsic variability of the source. The spectral index and the absorbing column density do not appear to have changed within the uncertainties.

We have compared our measurements with published reports of the spectrum of Pictor A measured in the 1980s with the *Einstein*/IPC and *EXOSAT*/ME+LE by Singh, Rao, & Vahia (1990). The results of these early observations are included in the second part of Table 2. A simple power-law model provides the best description of the *EXOSAT* and *Einstein* spectra, just as it does for the *ASCA* and *ROSAT* spectra. Also included in Table 2 are the spectral parameters measured by Brinkmann & Siebert (1994) from the RASS data. The soft (0.7–2.4 keV) X-ray flux varies by less than a factor of 3 over all observations of Pictor A to date. The spectral shape and

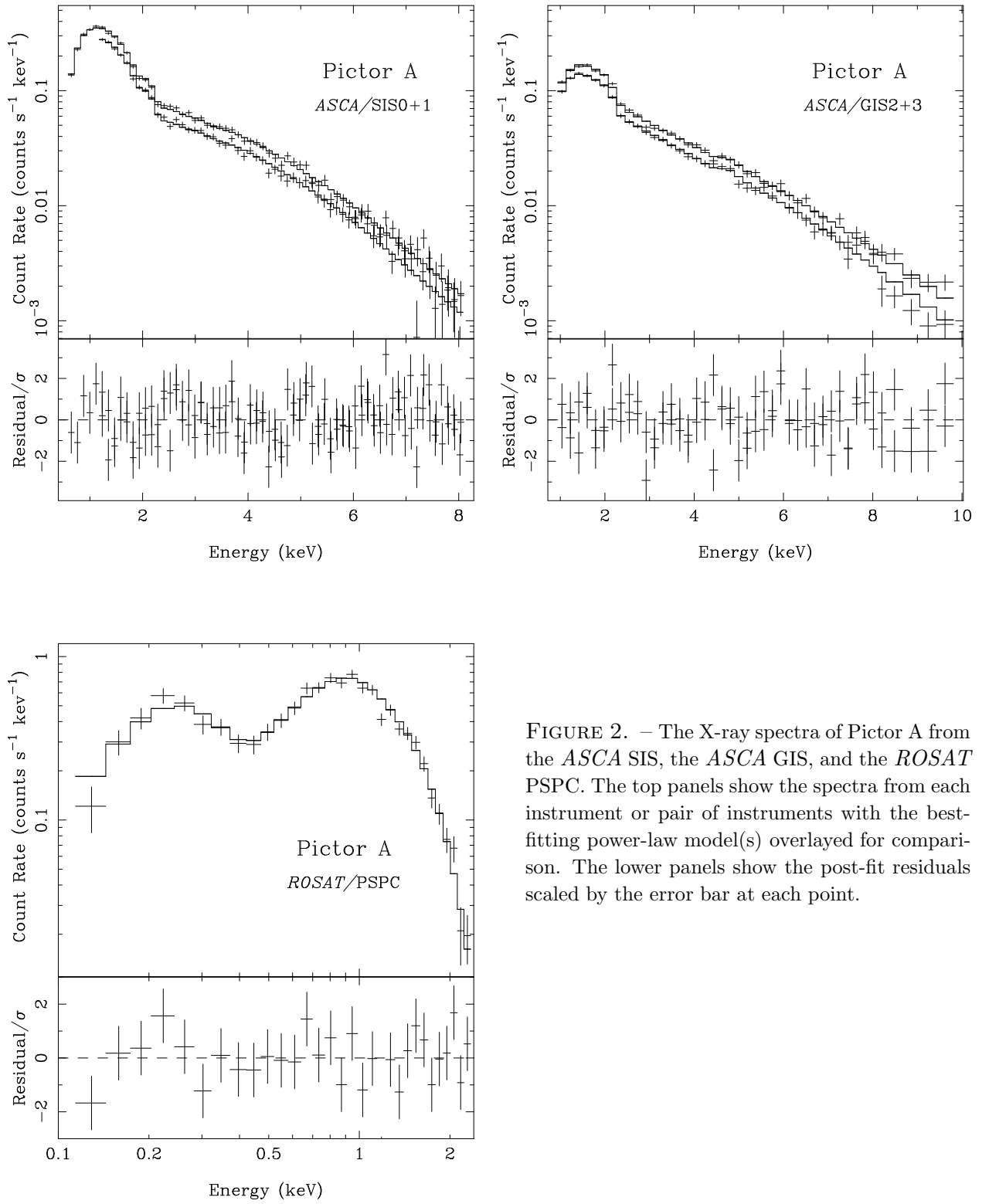


FIGURE 2. – The X-ray spectra of Pictor A from the *ASCA* SIS, the *ASCA* GIS, and the *ROSAT* PSPC. The top panels show the spectra from each instrument or pair of instruments with the best-fitting power-law model(s) overlaid for comparison. The lower panels show the post-fit residuals scaled by the error bar at each point.

TABLE 2: BEST-FITTING MODEL PARAMETERS AND FLUXES

Instrument	Year	χ^2_ν /d.o.f.	Photon Index ^a	Column Density ^a (10^{20} cm $^{-2}$)	Flux ^b (10 $^{-11}$ erg cm $^{-2}$ s $^{-2}$)	
					0.7–2.4 keV	2–10 keV
Measurements from This Paper						
<i>ASCA</i> /SIS 0 + 1	1996	1.066/106	$1.77^{+0.04}_{-0.05}$	6 ± 2	0.77 ± 0.03	1.4 ± 0.1
<i>ASCA</i> /GIS 2 + 3	1996	1.254/82	$1.76^{+0.06}_{-0.05}$	8 ± 4	...	1.5 ± 0.2
<i>ROSAT</i> /PSPC	1991	0.832/26	$1.7^{+0.3}_{-0.2}$	$4.4^{+1.6}_{-0.9}$	1.8 ± 0.2	...
Measurements from the Literature						
<i>ROSAT</i> /PSPC	1990 ^c	...	2.3 ± 0.6	7 ± 3	$1.94^{+0.12}_{-0.06}$...
<i>EXOSAT</i> /ME+LE	1986 ^d	...	1.8 ± 0.3	7^{+7}_{-4}	1.03 ± 0.06	1.73 ± 0.10
<i>Einstein</i> /IPC	1980 ^d	...	$1.5^{+0.5}_{-0.3}$	6^{+14}_{-4}	0.71 ± 0.03	...

^a The uncertainty in the model parameters corresponds to the 99% confidence limits for 2 interesting parameters.

^b The quoted flux has been corrected for interstellar photoelectric absorption. The error bars reflect the uncertainties in both the spectral index and the normalization.

^c RASS observation reported by Brinkmann & Siebert (1994)

^d Singh et al. (1990). The *Einstein* IPC flux has also been published by Kruper, Urry, & Canizares 1990.

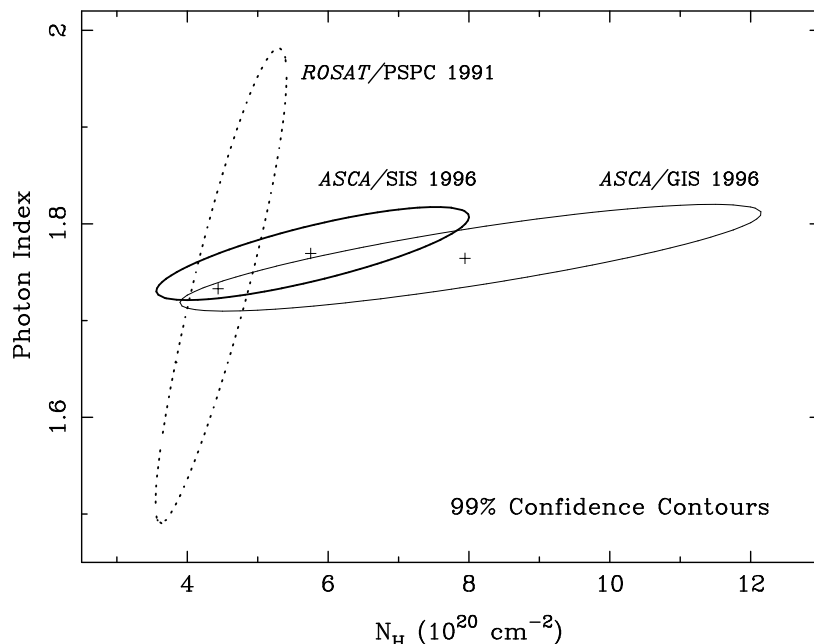


FIGURE 3. – The 99% confidence contours showing the correlated uncertainties between the power-law index and the column density of the best-fitting model for each instrument. The cross near the center of each contour marks the best fit obtained for that instrument.

absorbing column density do not appear to have changed (within uncertainties, of course). Since the X-ray spectrum between 0.5 and 10 keV is described well by a power law, it is reasonable to conclude that the 2–10 keV flux follows the variations of the soft X-ray flux. Finally, we note that the Galactic hydrogen column in the direction of Pictor A is $4.2 \times 10^{20} \text{ cm}^{-2}$ (Heiles & Cleary 1979). This is consistent, within errors, with all measurements of the absorption from the X-ray spectra, suggesting that the interstellar medium of the Galaxy is responsible for most of the observed absorption.

3.2 The Fe K α Line: Too Weak to Be Measurable

A ubiquitous feature in the *ASCA* X-ray spectra of Seyfert galaxies is an Fe K α line at a rest energy of 6.4 keV (see §1). This line is thought to arise by fluorescence in the same cool, dense matter where Compton reflection of the continuum takes place. Our preliminary inspection of the spectrum showed no evidence for a line. Hence, to investigate whether a weak line is present and to set limits on its equivalent width (hereafter *EW*) we fitted the *ASCA* spectra in the range 3.0–8.0 keV with a model consisting of a power-law continuum and a line. Photoelectric absorption was not included because its effects are negligible at column densities as low as what was measured in §3.1. We carried out the exercise under two different assumptions for the profile of the line. The first assumption is that the line has a Gaussian profile. The full velocity width of the line at half maximum, in its rest frame, is given by $FWHM = \sqrt{8 \ln 2} c \sigma_{\text{obs}}/E_{\text{obs}}$, where E_{obs} and σ_{obs} are the observed energy and energy dispersion of the line. The second assumption is that the line profile is disk-like, computed according to the model of Fabian et al. (1989). In this model the line originates in an annulus of a disk which is inclined to the line of sight and whose emissivity varies with radius as a power law. Motivated by the properties of Fe K α line in Seyfert galaxies, we have fixed the inner and outer radius of the line-emitting part of the disk to $6 r_g$ and $1000 r_g$ and set the emissivity proportional to r^{-3} in our implementation of this model. Thus, the inclination angle of the disk, which is a free parameter, effectively controls the width of the line (roughly as $FWHM \propto \sin i$, where i is the disk inclination). The main difference between the two model profiles is that the Gaussian profile is symmetric, while the disk-like profile is skewed with the red wing more prominent than the blue.

We applied each of our assumed models to the data from each pair of instruments. The strategy we adopted was to fit the continuum to the data in two windows straddling the line (3.0–4.0 keV and 7.0–8.0 keV; at $z = 0.035$, the line is expected to appear at 6.18 keV) and freeze it. The two continuum windows were chosen in view of the fact that the Fe K α lines observed in the *ASCA* spectra of Seyfert galaxies are extremely broad, with extended red wings. After setting the continuum level, the line was added to the model which was fitted to the entire 3.0–8.0 keV range, allowing the line flux and width to vary freely. To determine the upper limit to the *EW* of the line allowed by the data we scanned the line width–intensity parameter plane (or inclination–intensity plane, in the case of the disk-like profile model) looking for sets of parameters that yielded a significantly better fit to the data compared to the simple continuum model. The result of this parameter-space search is a set of upper limits on the flux of line photons as a function of the line width or the inclination of the disk. Because the continuum was held fixed as the line parameters were varied, the flux of the line can be translated to an *EW* by a simple scaling. Therefore, we present our results in the form of upper limits on the line *EW* versus line width or disk inclination in Figure 4. In this form, the upper limits that we determine can be compared directly with the measured *EWs* of lines in Seyfert galaxies from the compilation of Nandra et al. (1997a). To this end we plot in Figure 4 the individual *EWs* measured in Seyferts by Nandra et al (1997a) *along with their error bars*. We note that the method we have used here to determine the *EW* upper limits is not necessarily the same as that used by other authors to determine error bars in the *EW*

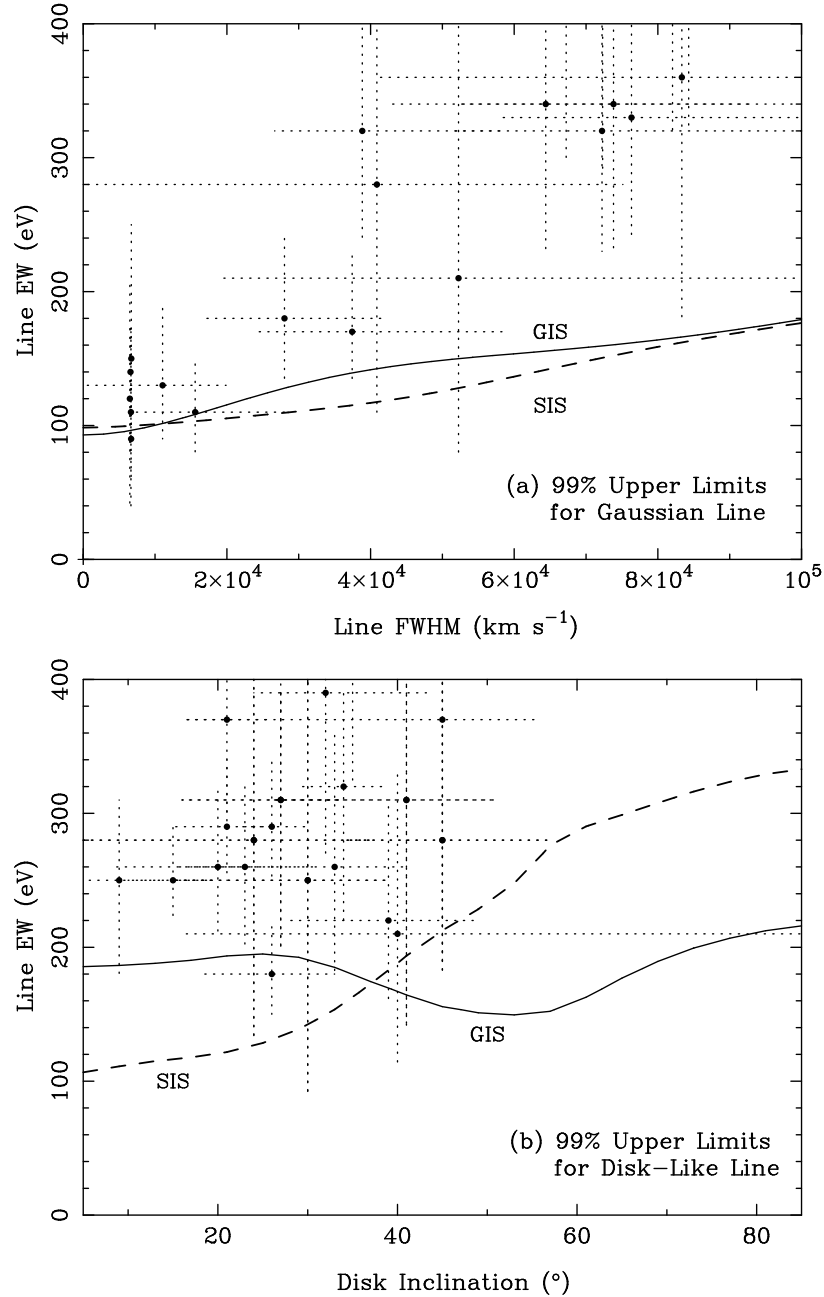


FIGURE 4. – (a) The upper limit to the Fe K α EW (measured in the observer’s frame) as a function of the $FWHM$ of the Gaussian profile assumed for the line. For reference, we note that the resolution of the SIS corresponds to a $FWHM$ of $12,700 \text{ km s}^{-1}$, and that of the GIS to $22,800 \text{ km s}^{-1}$. (b) The upper limit to the Fe K α EW (measured in the observer’s frame) as a function of disk inclination in the case where the line is assumed to have a disk-like profile. The inclination of the disk effectively controls the width of the line. In each panel we also plot the EW s and velocity widths measured in individual Seyfert galaxies by Nandra et al. (1997a) for comparison. Error bars for each measurement are also plotted as dotted lines in order to make the comparison as fair as possible.

of *detected* lines. The difference lies in that we have fixed the continuum level and allowed only the line parameters to vary freely. It is possible to allow the continuum level to be free as well, as other authors may have done, which would make the error bars on the line EW somewhat larger. Since we are interested in comparing the EW *upper* limits deprived here with the *lower* EW error bars deprived for Seyfert galaxies, the difference in methodology will not affect our conclusions.

The upper limit (at 99% confidence for 2 interesting parameters) to the observed EW of a line which is unresolved by the SIS (i.e., $FWHM < 1.28 \times 10^4 \text{ km s}^{-1}$) is 100 eV. For a resolved Gaussian line (either in the SIS or the GIS) the EW upper limit is a function of the width of the line. This is a manifestation of the fact that for a fixed EW a broader line can hide in the noise more easily than a narrower one. Moreover, the minimum detectable EW for a fixed exposure time with any given instrument is determined by the competition between its effective area and its spectral resolution. At the off-axis angles at which Pictor A was observed the effective area of GIS 3 at 6.2 keV is 25% higher than that of SIS 0. Therefore, the minimum detectable EW in the GIS is comparable to that in the SIS even though the spectral resolution of the former is almost a factor of 2 poorer than that of the latter (the exposure time in the GIS is also about 12% longer than in the SIS). For a Gaussian line that is as broad as the lines detected in Seyferts by Nandra et al. (1997a) the EW upper limit is 135 eV, assuming that $FWHM \approx 6 \times 10^4 \text{ km s}^{-1}$. This is below the range of EW measured in Seyferts under the same assumptions, as shown in Figure 4a. If the line is assumed to have a disk-like profile, the EW upper limit depends on the assumed inclination of the disk since this determines the width of the line. Figure 4b shows the relation between the the EW upper limit and the disk inclination for both the SIS and the GIS. If the disk inclination is assumed to be comparable to that measured for Seyferts by fitting their line profiles, the implied EW upper limit for Pictor A is 180 eV, which is well below the range of Seyfert galaxy EW s. We note that for assumed disk inclinations above 35° the resulting model line profiles are so broad that the higher sensitivity of the GIS compared to the SIS outweighs its poor spectral resolution and makes the EW limits from the former instrument more stringent than those from the latter.

4. DISCUSSION

4.1. Comparison With Other BLRGs and With Seyferts

The absence of an Fe K α line from the spectrum of Pictor A is surprising because such lines are detected in the spectra of almost all Seyfert 1 galaxies and BLRGs observed by *ASCA* (Nandra et al. 1997a; see also Table 3). We note that Singh et al. (1990) found a very strong Fe K α line in the *EXOSAT* spectrum of Pictor A ($EW \sim 1 \text{ keV}$) but those data could well be affected by systematic errors associated with the background at energies higher than 6 keV. To explore the implications of the weakness of the line we compare our limits on the line properties with the properties of lines detected in other BLRGs and in Seyferts. We also investigate whether the weakness of the line can be understood in the context of the known anticorrelation between X-ray luminosity and Fe K α EW (Nandra et al. 1997b). To this end we collect in Table 3 information of the properties of Fe K α lines of BLRGs from the literature. We include in this table constraints on the the inclination angle of the jet (and hence the disk) of each object derived from its radio properties. Namely, (a) we obtain a *lower* limit on the jet inclination by requiring that the size of the double-lobed radio source not exceed the largest sizes observed in radio galaxies, and (b) for three objects displaying superluminal motion we obtain an *upper* limit on the jet inclination from the measured superluminal speed (see the detailed discussion of the method by Eracleous et al. 1996). In Figure 5 we plot the Fe K α rest-frame EW s of BLRGs against luminosity, and we also indicate the region of this diagram occupied by Seyferts, according to Nandra et al. (1997b), for

TABLE 3: BLRG IRON LINE PROPERTIES

Object	z	L_x (2–10 keV) (erg s $^{-1}$)	Rest EW (eV)	$FWHM$ (10 3 km s $^{-1}$)	Inclination	References ^a
3C 109	0.306	2.1×10^{45}	390_{-260}^{+780}	90_{-50}^{+112}	$i > 35^\circ$	1,2
3C 111 ^b	0.048	4.1×10^{44}	< 130	...	$37^\circ > i > 24^\circ$	2,3,4,5
3C 120 ^c	0.033	2.0×10^{44}	380_{-140}^{+100}	91_{-35}^{+34}	$14^\circ > i > 1^\circ$	6,7,8
Pictor A	0.035	7.9×10^{43}	< 140	...	$i > 24^\circ$	2,9,10
3C 382	0.059	6.0×10^{44}	950_{-320}^{+1100}	197_{-55}^{+109}	$i > 15^\circ$	2,11
3C 390.3	0.056	2.0×10^{44}	190_{-70}^{+100}	15_{-8}^{+15}	$33^\circ > i > 19^\circ$	2,12,13
3C 445	0.057	8.5×10^{43}	270_{-90}^{+130}	18_{-14}^{+18}	$i > 60^\circ$	14,15

^a References: (1) Allen et al. 1997; (2) Nilsson et al. 1993; (3) Reynolds et al. 1997; (4) Eracleous & Halpern 1997b; (5) Vermuelen & Cohen 1994; (6) Grandi et al. 1997; (7) Balick, Heckman & Crane 1982; (8) Zensus 1989; (9) this work; (10) Jones & McAdam 1992; (11) Reynolds 1997; (12) Eracleous et al. 1996; (13) Alef et al. 1994; (14) Sambruna et al. 1997; (15) McCarthy, van Breugel, & Kapahi 1991.

^b Reynolds et al. (1997) report a marginal detection of an Fe K α line with an $EW \approx 100$ eV under the assumption of a disk-like profile. Our own independent analysis of the same data (Eracleous & Halpern 1998b) yielded an upper limit to the EW of a Gaussian line of 130 eV, which we adopt here.

^c The upper limit on the inclination of the jet in 3C 120, $i < 14^\circ$, is based on a superluminal speed of $\beta_{app}=8.1$, reported by Zensus (1989). Other authors (Wehrle et al. 1992; Walker, Walker, & Benson 1988) report lower superluminal speeds ($\beta_{app} = 4.1$ and $\beta_{app} = 3.7 \pm 1.2$, respectively), which imply $i \lesssim 25^\circ$.

comparison (the width of the grey band in this figure corresponds to the dispersion in the EW of objects in the same luminosity bin).

Figure 5 has a number of interesting and noteworthy features. First, with the exception of 3C 109 (which is best classified as a quasar rather than a BLRG because of its high luminosity) all objects cluster in a narrow luminosity range around 10 44 erg s $^{-1}$. Second, there is a large scatter in EWs among BLRGs, ranging from < 130 eV (3C 111) to > 600 eV (3C 382). Third, the large EWs observed in 3C 120 and 3C 382 are particularly disturbing (or interesting, depending on one's perspective) if they are considered in combination with the line widths ($FWHM$). As the authors who report the original results point out (Reynolds 1997; Grandi et al. 1997) the lines are so broad that it is difficult to understand their widths in the context of a line-emitting disk model for their origin. In the case of 3C 120, the disk is thought to be viewed almost face-on ($i < 14^\circ$) and yet its Fe K α line has an *observed FWHM* of 91,000 km s $^{-1}$. If this is true, then the intrinsic (deprojected) velocities of the line wings should exceed the speed of light. In the case of 3C 382 the *observed FWHM* corresponds to half the speed of light, implying that the wings of the line should correspond to superluminal speeds regardless of the inclination. We note that such large widths and EWs could have come about if the continuum level was underestimated in the original analysis of the data. Such a problem can come about if, for example, the continuum level is allowed to vary freely when fitting the line. Under these conditions a very broad line can mimic the continuum and result in an erroneous estimate of the equivalent width. Indeed, Woźniac et al. (1998) find from their independent analysis of the same data that the lines are weaker and narrower than the original

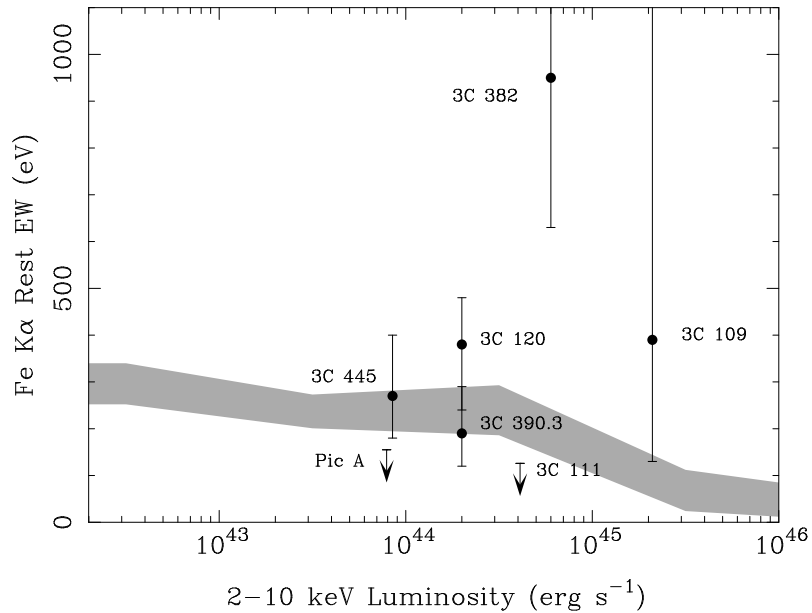


FIGURE 5. – The rest-frame *EWs* of the Fe K α lines of BLRGs plotted against luminosity. The data themselves are given in Table 3. The shaded band shows the region of the *EW*-luminosity plane occupied by Seyfert galaxies according to Nandra et al. 1997b. The width of this band reflects the dispersion in *EWs* among objects in the same luminosity bin. In the highest luminosity bin the sample of Nandra et al. (1997b) includes a significant number of radio-loud objects.

reports suggest. However, since the results of Woźniac et al. (1998) are not yet published, we take the reported line properties at face value, but we regard them with great caution. The moral of this comparison is that the orientation of the disk (or the jet) does not seem to play an important role in determining the properties of the Fe K α line. We reach this conclusion by considering the fact that both 3C 390.3 and 3C 445 which have very different jet inclinations have relatively weak and narrow lines, while 3C 382 and 3C 120 also have very different inclinations and yet have very strong lines and very broad. With this observation in mind we turn our attention to possible reasons for the weakness of the Fe K α line in Pictor A, which we discuss in the next section.

4.2. What Happened to the Fe K α Line?

Production of the fluorescent Fe K α line requires that an X-ray continuum illuminates cold target material of sufficient optical depth and covering fraction. In ordinary Seyfert galaxies, it is thought that the only target with the necessary properties is the accretion disk. In the context of this scenario we consider possible reasons for the weakness of the Fe K α line in Pictor A. We seek an explanation which is not just specific to Pictor A, but rather one that is also consistent with all (or at least most) of the available data as they are summarized in Table 3, including the widths of the Fe K α lines and the independent information on the disk orientation obtained from the radio properties.

- (a) *A Highly Inclined Disk:* The inclination angle of the accretion disk of Pictor A is likely to be large. The radio core-to-lobe luminosity ratio ($\log R = -1.82$; Jones & McAdam 1992) and the projected separation of the radio lobes (Table 3) imply $i > 24^\circ$. If this is the case, then there are two effects which conspire to hide the line. First, the EW of the line predicted by models is a function of the disk inclination; at $i = 50^\circ$ it is 30% smaller than the face-on value (George & Fabian 1991; Matt et al. 1991). Second, the line appears broader if the disk is viewed at a higher inclination, and hence for a fixed line flux the EW threshold for detecting it increases ($EW_{\min} \propto FWHM \propto \sin i$). This interpretation is consistent with the lack of a Compton-reflected spectral component at the highest observable energies. However, the same explanation *cannot* be invoked for 3C 111 or 3C 390.3 whose superluminal motion and projected radio lobe separation require that their disks are viewed close to face on (Table 3). Moreover, 3C 109 does not fit into the picture either because it has a strong line although the inclination of its disk appears to be large.
- (b) *Inner Disk Structure Different from Seyferts:* Production of the large equivalent widths in Seyfert galaxies is difficult to achieve in an accretion disk geometry unless the covering fraction is close to 50%. This requires the hard X-ray source to “hug” the accretion disk, as would a geometrically thin corona. BLRGs could have a different accretion disk structure, such as a spherical corona above a thin disk, or an ion torus that results from an instability in the inner disk (within a few hundred r_g). In the latter case, the covering fraction of the cold outer disk as seen by the X-ray source is at most 25%, and possibly considerably less than that, as shown by simple geometrical considerations (Chen & Halpern 1989). Moreover, the Keplerian velocity in the line-emitting part of the disk is only around $10,000\text{--}30,000 \text{ km s}^{-1}$, with the consequence that the observed lines in BLRGs should be narrower than in Seyferts. This idea is analogous to the scenario put forth by Woźniac et al. (1998) in which the Fe K α lines were produced in medium far away from the central black hole whose column density was not high enough to give rise to Compton reflection. Here, however, we make the specific suggestion that the medium where the lines originate is the outer accretion disk itself. This explanation could also apply to 3C 390.3, whose Fe K α line is neither as broad nor as strong as those of Seyferts, and perhaps also to 3C 445. However, the same explanation would not apply to objects such as 3C 109, 3C 120, or 3C 382 which seem to have strong, broad Fe K α lines.
- (c) *Continuum Beamed Away from the Disk:* The observed continuum could be beamed in a direction away from the accretion disk, the latter being the source of Fe K α lines in Seyferts. The result is that the disks of BLRGs are not illuminated effectively and hence their lines are weak. However, they may still have weak narrow Fe K α lines if the continuum illuminates part of the broad-line region (Yaqoob et al. 1993). But this would appear to be a rather contrived explanation because it applies only to Pictor A and 3C 111. Most BLRGs observed with *ASCA* do have broad Fe K α lines (some are quite strong) and there is no obvious correspondence between their continuum luminosity and the orientation of their disks; hence they do not support this hypothesis.
- (d) *Continuum Beamed Towards the Observer:* If the observed continuum is beamed towards the observer (presumably because the source is associated with the jet), then the continuum level is boosted and the observed EW of an unbeamed line decreases. However, the jet orientation arguments presented in (a) above make this an unlikely explanation for Pictor A. For an assumed jet Lorentz factor of 10, the only object in Table 3 for which beaming could boost the continuum flux by a large factor is 3C 120. In the case of 3C 382 a modest enhancement of the continuum by a factor of a few is possible. For all other objects the jet inclination angles are such that beaming does not have the desired effect. Hence the presence a beamed continuum source seems like an unlikely explanation for the weakness of the lines.

(e) *Low Iron Abundance*: The observed Fe K α equivalent width decreases with the Fe abundance, thus a low Fe abundance in the disk could result in weak Fe lines. However, there is no good motivation for assuming that the accretion disk is Fe poor. On the other hand, an Fe deficit as small as a factor of 2 relative to Seyfert galaxies can bring about the observed effect. If we take the observed widths of the Fe K α lines in BLRGs at face value, then the profiles of Fe K α lines of BLRGs are no different than those of Seyferts. It could, therefore, be argued that the entire range of Fe K α *EWs* observed in BLRGs (and Seyferts) can be attributed to variations in the Fe abundance between objects by a factor of a few. If however, the Fe K α lines of BLRGs are systematically narrower than those of Seyferts, then the Fe abundance cannot be the only difference between the two classes of object.

Another aspect of the puzzle of the weak Fe K α line in Pictor A is why there is no Fe K α emission from the gas that emits the double-peaked Balmer lines. The displaced peaks appear only in the Balmer lines and *not* in the ultraviolet lines (i.e., Ly α , C IV, C III]; Eracleous et al., in preparation). In particular the upper limit to the Ly α /H β ratio in the displaced peaks is 0.25, suggesting that the medium where the double-peaked lines originate is dense with a high column density ($N_{\text{H}} \gtrsim 10^{24-25} \text{ cm}^{-2}$) and a low ionization parameter ($U \lesssim 10^{-3}$; Halpern et al. 1996; Collin-Souffrin & Dumont 1989)⁴. It is therefore paradoxical that the same medium is not a strong source of Fe K α emission, unless it subtends a very small solid angle to the primary X-ray source (e.g., it has the form a thin ring or a pair of narrow jets).

In the optically thin limit, the observed upper limit to the *EW* sets the following limit on the product of the column density of the line-emitting gas and its covering fraction:

$$N_{\text{H}} f_{\text{c}} < 1.6 \times 10^{23} \left(\frac{\text{EW}}{140 \text{ eV}} \right) \left(\frac{4 \times 10^{-5}}{A_{\text{Fe}}} \right) \text{ cm}^{-2}, \quad (1)$$

where A_{Fe} is the iron abundance. Equation (1) suggests that either the covering fraction of the medium responsible for the double-peaked Balmer lines of order 0.01–0.1, or the Fe abundance is low. This requirement, along with the abrupt appearance of the double-peaked Balmer lines, supports the hypothesis that they come from a region which is dynamically and physically distinct from the “normal” broad-line region. Unfortunately, it is difficult to make more progress in our quest for the origin of the double-peaked lines before we can distinguish between the two possible reasons for the weakness of the Fe K α line mentioned above. Hard X-ray spectra provide a way out of this impasse, as we discuss briefly in the next section.

5. CONCLUSIONS, SPECULATIONS, AND FUTURE PROSPECTS

The lack of an Fe K α line in the X-ray spectrum of Pictor A is surprising because this line is ubiquitous in the X-ray spectra of other BLRGs and of Seyfert galaxies. We have considered several possible explanations for the weakness of the line, none of which is quite satisfactory, with the possible exception of a low Fe abundance. An important shortcoming of all other candidate explanations is that they do not offer a framework in which the Fe K α properties of *all* BLRGs observed with *ASCA* can be understood. We have argued that the extremely broad Fe K α lines observed in some of the BLRGs are a cause for concern since the velocity of the line wings can exceed the speed of light. The problem could be the consequence of underestimating the continuum level in the vicinity of the line. This suggestion is supported by the fact that a re-analysis of the data

⁴ The photoionization models of Rees, Netzer, & Ferland (1989), which assume $N_{\text{H}} = 10^{23} \text{ cm}^{-2}$ and $U = 10^{-2}$ cannot produce Ly α /H β ratios less than 10!

by Woźniac et al. (1998) has yielded different results from the original analysis (i.e., narrower and weaker lines, in general). We have also embarked on an independent analysis of all of the available data (Sambruna, Eracleous, & Mushotzky 1998), in order to verify the findings of Woźniac et al. (1998).

Assuming that the Fe K α lines of BLRGs turn out to be weaker than those of Seyfert galaxies, as the preliminary results of the two groups, above, suggest, then another one of the candidate explanations examined in §4.2 becomes promising: the accretion disks of BLRGs may have a different structure than those of Seyferts. If reliable information on the line widths (and profiles) can be obtained from the *ASCA* SIS spectra, it can be used to discriminate between the two explanations (different disk structure and different Fe abundance). If the Fe K α lines of BLRGs are systematically narrower than those of Seyferts, the structure explanation would be favored over the abundance hypothesis. Alternatively, hard X-ray spectra can be used to discriminate between the two possibilities by measuring the strength of the Compton reflection hump. If the Fe abundance is low, the optical depth above the Fe K edge at 7.1 keV is small and the contrast of the Compton reflection hump is higher (e.g., George & Fabian 1991; Reynolds et al. 1995). If, however, the weakness of the line is the result of a small covering fraction of the reprocessing medium, the contrast of the Compton reflection hump decreases along with the strength of the line. We note in conclusion that a picture in which the X-ray reprocessing medium in Pictor A is a narrow ring of gas with a large column density and a small covering fraction is aesthetically very pleasing. Its appeal lies in that it can explain all of the spectroscopic properties at the same time, including the relative strengths and profiles of the optical and ultraviolet lines and the weakness of the Fe K α line.

We are grateful to R. Sambruna and A. Zdziarski for very useful discussions and the anonymous referee for thoughtful comments. We also thank C. Reynolds for sending us the manuscript of his paper on the *ASCA* observations of 3C 111 ahead of publication. M. E. acknowledges support from Hubble fellowship grant HF-01068.01-94A from Space Telescope Science Institute, which is operated for NASA by the Association of Universities for Research in Astronomy, Inc., under contract NAS 5-26255. This work was also supported by NASA grant NAG 5-2524.

REFERENCES

Alef, W., Preuss, E., Kellerman, K. I., Wu, S. Y., & Qiu, Y. H. 1994, in Compact Extragalactic Radio Sources, NRAO Workshop No. 23, eds. J. A. Zensus & K. I. Kellerman (Green Bank: NRAO), 55

Allen, S. W., Fabian, A. C., Idesawa, E., Inoue, H., Kii, T., & Otani, C. 1997, MNRAS, 286, 765

Arnaud, K. A. 1996, in “Astronomical Data Analysis Software and Systems V”, eds. G. Jacoby & J. Barnes, ASP Conf. Series, 101, 17

Balick, B., Heckman, T. M., & Crane, P. C. 1982, ApJ, 254, 483

Blackburn, J. K., Greene, E. A., & Pence, B. 1994, User’s Guide to FTOOLS (Greenbelt: Goddard Space Flight Center)

Brinkmann, W. & Siebert, J. 1994, A&A, 285, 812

Chen, K., & Halpern, J. P. 1989, ApJ, 344, 115

Collin-Souffrin, S., & Dumont, A. M. 1989, A&A, 213, 39

Corbin, M. R. 1997, ApJ, 485, 517

Eracleous, M. & Halpern, J. P. 1994, ApJS, 90, 1

———. 1998a, in preparation

_____. 1998b, in “Accretion Processes in Astrophysical Systems: Some Like it Hot”, eds. S. S. Holt & T. R. Kallman (New York: ASP), in press

Eracleous, M., Halpern, J. P., & Livio, M. 1996, *ApJ*, 459, 89

Fabian, A. C., Rees, M. J., Stella, L., & White, N. E. 1989, *MNRAS*, 238, 729

George, I. M., & Fabian, A. C., 1991, *MNRAS*, 249, 352

George, I. M., Nandra, K., & Fabian, A. C. 1990, *MNRAS*, 242, 28P

Grandi, P., Sambruna, R. M., Maraschi, L., Matt, G., Urry, C. M., & Mushotzky, R. F., 1997, *ApJ*, 487, 636

Guilbert, P. W., & Rees, M. J. 1988, *MNRAS*, 233, 475

Haardt, F., & Maraschi, L. 1991, *ApJ*, 308, L51

_____. 1993, *ApJ*, 413, 507

Haardt, F., Maraschi, L., & Ghisellini, G. 1994, *ApJ*, 432, L95

Halpern, J. P., Eracleous, M., Filippenko, A. V., & Chen, K. 1996, *ApJ*, 467, 704

Halpern, J. P., & Eracleous, M. 1994, *ApJ*, 433, L17

Heiles, C. & Cleary, M. N. 1979, *AuJPA*, 47, 1

Ingham, J. 1994, The XSELECT User’s Guide (Greenbelt: Goddard Space Flight Center)

Jackson, N., & Browne, I. W. A. 1991, *MNRAS*, 250, 414

Jackson, N., Penston, M. V., & Pérez, E. 1991, *MNRAS*, 248, 577

Jones, P. A., & McAdam, W. B. 1992, *ApJS*, 80, 137

Kruper, J. S., Urry, C. M., & Canizares, C. R. 1990, *ApJS*, 74, 347

Lightman, A. P., & White, T. R. 1988, *ApJ*, 335, 57

Magdziarz, P., & Zdziarski, A. A. 1995, *MNRAS*, 273, 837

Matt, G., Perola, G. C., & Piro, L. 1991, *A&A*, 247, 2

McCarthy, P., van Breugel, W., & Kapahi, V. J. 1991, *ApJ*, 371, 478

Miley, G. K., & Miller, J. S. 1979, *ApJ*, 228, L55

Morrison, R. & McCammon, D. 1983, *ApJ*, 270, 119

Mushotzky, R. F. et al. 1995, *MNRAS*, 272, P9

Nandra, K., & George, I. M. 1994, *MNRAS*, 267, 974

Nandra, K., George, I. M., Mushotzky, R. F., Turner, T. J., & Yaqoob, T. 1997a, *ApJ*, 477, 602

_____. 1997b, *ApJ*, 488, L91

Nandra, K., & Pounds, K. A. 1994, *MNRAS*, 268, 405

Narayan, R. & Yi, I. 1994, *ApJ*, 428, L13

Narayan, R. & Yi, I. 1995, *ApJ*, 444, 231

Nillson, K., Valtonen, M. J., Kotilainen, J., & Jaakkola, T. 1993, *ApJ*, 413, 453

Pounds, K. A., Nandra, K., Stewart, G. C., & Leighly, K. 1989, *MNRAS*, 240, 769

Rees, M. J., Begelman, M. C., Blandford, R. D., & Phinney, E. S. 1982, *Nature*, 295, 17

Reynolds, C. S. 1997, *MNRAS*, 286, 513

Reynolds, C. S., Iwasawa, K., Crawford, C. S., & Fabian, A. C. 1997, *MNRAS*, in press

Reynolds, C. S., Fabian, A. C., & Inoue, H. 1995, *MNRAS*, 276, 1311

Sambruna, R. M., Eracleous, M., & Mushotzky, R. F. 1998, in preparation

Sambruna, R. M., George, I. M., Mushotzky, R. F., Nandra, K., & Turner, T. J. 1997, *ApJ*, in press

Sinclair, M. W. & Krolik, J. H. 1997, *ApJ*, 476, 605

Singh, K. P., Rao, A. R., & Vahia, M. N. 1990, *MNRAS*, 246, 706

Steiner, J. E. 1981, *ApJ*, 250, 469

Sulentic, J. W., Marziani, P., Zwitter, T., & Calvani, M. 1995, *ApJ*, 438, L1

Tanaka, Y., Inoue, H., & Holt, S. S. 1994, *PASJ*, 46, L37

Tanaka, Y., et al. 1995, *Nature*, 375, 659

Turner, T. J. & Pounds, K. A. 1989, *MNRAS*, 232, 463

Vermuelen, R. C., & Cohen, M. H. 1994, *ApJ*, 430, 467
Walker, R. C., Walker, M. A., & Benson, J. M. 1988, *ApJ*, 335, 668
Wehrle, A. E., Cohen, M. H., Unwin, S. C., Aller, H. D., Aller, M. F., & Nicolson, G. 1992, *ApJ*, 391, 589
Wills, B. J., & Browne, I. W. A. 1986, *ApJ*, 302, 56
Woźniac, P. R., Zdziarski, A. A., Smith, D., Madejski, G. M., & Johnson, W. N. 1998, *MNRAS*, in press
Yaqoob, T. 1996, in “Minutes of *ASCA* Calibration Meeting, ISAS, 1996 Nov. 16”
Yaqoob, T., McKernan, B., Done, C., Serlemitsos, P. J., & Weaver, K. A. 1993, *ApJ*, 416, L5
Zdziarski, A. A., Johnson, W. N., Done, C., Smith, D., & McNaron-Brown, K. 1995, *ApJ*, 438, L63
Zensus, J. A. 1989, in *Lecture Notes in Physics* vol. 334 “BL Lac Objects”. eds. L. Maraschi, T. Maccacaro, & M.-H. Ulrich (Berlin: Springer), 3